Debromination of Decabrominated Diphenyl Ether by Resin-Bound Iron Nanoparticles

ARTICLE *in* ENVIRONMENTAL SCIENCE AND TECHNOLOGY · NOVEMBER 2007

Impact Factor: 5.33 · DOI: 10.1021/es070769c · Source: PubMed

Debromination of Decabrominated Diphenyl Ether by Resin-Bound Iron Nanoparticles

AN LI,[†,‡] CHAO TAI,[†] ZONGSHAN ZHAO,[†,§] YAWEI WANG,[†] QINGHUA ZHANG,[†] GUIBIN JIANG,*[,†] AND JINGTIAN HU[§]

State Key Laboratory of Environmental Chemistry and Ecotoxicology, Research Center for Eco-Environmental Sciences, Chinese Academy of Sciences, Beijing, China, School of Public Health, University of Illinois, Chicago, Illinois, and Department of Chemistry, Shandong University, Jinan, China

Nanoscale zerovalent iron, n-ZVI, was found to be highly effective in reductively debrominating decabromodiphenyl ether (BDE209) at ambient conditions and without the catalysis of noble metals. A method was developed to immobilize n-ZVI particles on a cation-exchange resin. The n-ZVI coated resin was then mixed with BDE209 in a water/acetone (1:1) solution, and the reaction was allowed to proceed for up to 10 days. The first-order rate constant of BDE209 disappearance was estimated to be 0.28 ± 0.04 h^{-1}. The debromination was found to be stepwise, and less-brominated congeners were produced with increasing reaction time. Dechlorination of decachlorobiphenyl (PCB209) was also investigated, but the reaction rate was much slower than the debromination of BDE209. Identification of the reaction products was highly challenging and was assisted by regression equations between experimental and reference gas chromatographic relative retention times, with confirmation by high-resolution mass spectrometry and reference to quantitative structure retention relationships. For randomly selected PBDE and PCB congeners, the net charges of individual atoms were calculated using the quantum chemical computation to explore the difference in relative vulnerability of halogens at different substitution positions between PBDEs and PCBs.

Introduction

Polybrominated diphenyl ethers (PBDEs) have been widely used as flame retardants in numerous consumer products in the past three decades. Three PBDE technical mixtures were commercially available, but Deca is the only one currently produced in large quantities worldwide (*1*). The major component of Deca is decabromodiphenyl ether (BDE209), the fully brominated congener (*1*). From a chemical point of view, BDE209 is a labile molecule. Its formation is entropically unfavorable (*2*), and it has been found to debrominate to lower PBDE congeners under various natural or laboratory conditions (*3*−*7*). Such debromination may lead to the reduction and ultimate elimination of PBDEs in the environment but could meanwhile bring adverse ecological effects during the process because PBDE congeners with less than six bromines are more bioaccumulative and toxic than the parent BDE209 (*8*).

Knowledge on the reaction pathways, as well as of the kinetics, is therefore crucial to understand the toxicity of debromination products and the possible impact on the environment. It is well-known that the toxicity of halogenated aromatic compounds depends on not only the number but also the positions of the halogen atoms. For polychlorinated biphenyls (PCBs), relatively high resistance of ortho chlorines to dechlorination is observed in both laboratory and the field (*9*−*11*). For PBDEs, a few published debromination pathways suggest a different positional preference (*7*, *12*). The oxygen atom between the two rings renders PBDE molecules nonlinear and nonplanar (*2*). This may affect the relative vulnerability of bromines at different positions in various debromination processes.

Zerovalent iron (ZVI) is known to be a reducing agent for many organic compounds under anaerobic conditions. Its application in environmental remediation has targeted mainly chlorinated solvents, such as trichloroethene (TCE), in groundwater. Recently, remediation of soils and sediments contaminated by PCBs has also been carried out using ZVI (*13*, *14*). Halogenated aromatic compounds are intrinsically more stable than halogenated aliphatic ones. PCBs, for example, were found to be much more resistant to dechlorination than TCE (*15*). Rapid and efficient dechlorination of PCBs by ZVI has been observed at elevated temperatures or when the iron particles are palladized by deposition of a small amount of palladium on the iron surface as catalyst (*15*−*19*). Nanoscale (<100 nm id) ZVI (n-ZVI) was found to be more reactive than the ZVI with submicro- (100 nm to 1.0 μm) and micro- (1−50 μm) sizes (μ-ZVI) for the dechlorination of PCBs, most likely because of the higher surface reactivity on larger specific surface area (*20*). However, the size of the nanoparticles can be problematic for engineering practice. For example, particles of n-ZVI are highly reactive when exposed to air, enhancing the hazards of fire or explosion during storage and handling. Occupational safety and health are also important concerns because of nanotoxicity (*21*). It is recommended by the Royal Society of the U.K. that "the use of free (that is, not fixed in a matrix) manufactured nanoparticles in environmental applications such as remediation be prohibited until appropriate research has been undertaken" (*22*).

This study was initiated to investigate the feasibility of using n-ZVI to debrominate BDE209 in solution and the reaction pathways with respect to bromine substitution positions. An innovative method was developed to immobilize nanoscale iron particles on a cation exchange resin, and the application of this method may be well beyond the scope of this work. Experiments on BDE209 debromination using n-ZVI embedded on the resin were conducted. Predictive equations were developed to enhance the identification of reaction products. Efforts were made to propose debromination pathways, and the positional preference of bromine elimination is discussed. For comparison purposes, decachlorobiphenyl (PCB209) was tested for its dechlorination by n-ZVI, both coated on resins and suspended in solution, and the differences between BDE209 and PCB209 are explored.

Experimental Section

Chemicals. A small amount of marketed decabromodiphenyl ether product DE-83R was obtained as a gift of the Great Lakes Chemicals Co. (Indianapolis, IN). It is a solid white

* Corresponding author phone: 011-86-10-6284-9179; e-mail: gbjiang@mail.rcees.ac.cn.
† Chinese Academy of Sciences.
‡ University of Illinois at Chicago.
§ Shandong University.

powder with 97% purity and a theoretical 83.3% by mass of organic bromine content. It was used as BDE209 without further purification. A standard solution of PBDEs (EO5113) containing 39 PBDE congeners was purchased from Cambridge Isotope Laboratories (CIL, Andover, MA). BDEs 196, 197, 203, and 204 were obtained from Wellington Laboratories Inc. (Canada). Another standard solution (EO5103) containing 13 congeners was obtained from CIL. Table S1 of the Supporting Information contains the substitution patterns of the PBDE congener standards, as well as other congeners discussed in this paper. The solvent toluene was pesticide grade (Tedia Company, Fairfield, OH). Acetone and hydrochloric acid were from Beijing Chemical Co. (Beijing, China). Distilled water was used in all of the experiments.

Coating of n-ZVI on Ion-Exchange Resin. A method was developed to immobilize nanoscale iron particles on a cation-exchange resin (polystyrene, strong acid type) with the diameter ranging from 0.4 to 0.8 mm. The resin was purchased from Sinopharm Chemical Reagent Co., Ltd (Shanghai, China). Briefly, 2 g of $FeCl_2 \cdot 4H_2O$ was dissolved in 40 mL of distilled water; then 5 g of the resin was added. After the mixture was stirred for 2 h for the exchange of Fe^{2+}, the resin was separated from the solution and washed thoroughly with distilled water. Then, the resin was placed in 40 mL of 10 °C distilled water, and 20 mL of 10% (m/v) KBH_4 was added slowly with stirring to reduce the Fe^{2+}. After the mixture reacted for 0.5 h, the resin was separated and washed thoroughly to remove the residual KBH_4. The morphology of the resin and the iron particles were examined by HITACHI S-3000N scanning electron microscope (SEM).

Dehalogenation Experiments. About 50 test tubes (25 mL) were prepared, in which BDE209 in acetone was mixed with an equal volume of distilled water to form an 8 mL solution containing 0.1 μg mL^{-1} of BDE209. Then 2 g of resin (with 0.11 g n-ZVI coated except for the control samples) was added. The test tubes were capped with glass stoppers, sealed by Parafilm, and shaken for 1 h to 10 days in a water bath (25 ± 0.5 °C). At the preselected time intervals (0, 1, 2, 4, 8, and 24 h, followed by 24 h increments up to 240 h), triplicate sample tubes were taken. For each of them, the solution was poured into a 10 mL separating funnel and extracted by toluene (0.5 mL × 3). The resin was washed by toluene (1 mL × 3). The extract and eluent were combined. After they were dried on Na_2SO_4, the final volume was brought to 4.0 mL for instrumental analysis.

PCB209 was also investigated for its dechlorination by resin coated with n-ZVI using the same procedures as used for BDE209, but no reaction was evident after 10 days. To compare BDE209 and PCB209, a commercial aqueous suspension of n-ZVI (Toda Kogyo Corp., Japan) was diluted with distilled water and mixed with PCB209 in acetone in 5 mL test tubes to form 2 mL solutions containing 0.5 μg mL^{-1} of PCB209 and 0.125 g mL^{-1} of n-ZVI in 1:1 water/acetone. The test tubes were capped, sealed, and shaken in a manner similar to that described above. At the end of preset reaction times, ranging from 5 min to 10 days, triplicate sample tubes were taken, diluted by the addition of 5 mL of water and 1 mL of concentrated hydrochloric acid, and liquid−liquid extracted by toluene (0.5 mL × 3). After they were dried on Na_2SO_4, the three toluene portions were combined, and the final volume was adjusted to 2.0 mL for instrumental analysis.

Instrumental Analysis. An Agilent 6890II gas chromatograph (GC) with an ECD detector was used for PBDE analysis. Splitless 1 μL injection was performed manually at 300 °C. Most analyses used a DB-5 capillary column (15 m × 0.32 mm × 0.25 μm). The oven temperature was held initially at 150 °C for 2 min, increased at the rate of 15 °C min^{-1} to the final temperature of 325 °C, which was held for 7 min. Another DB-5 column (60 m long) was also used to enhance the separation of peaks and congener identification for 3 samples taken at different reaction times.

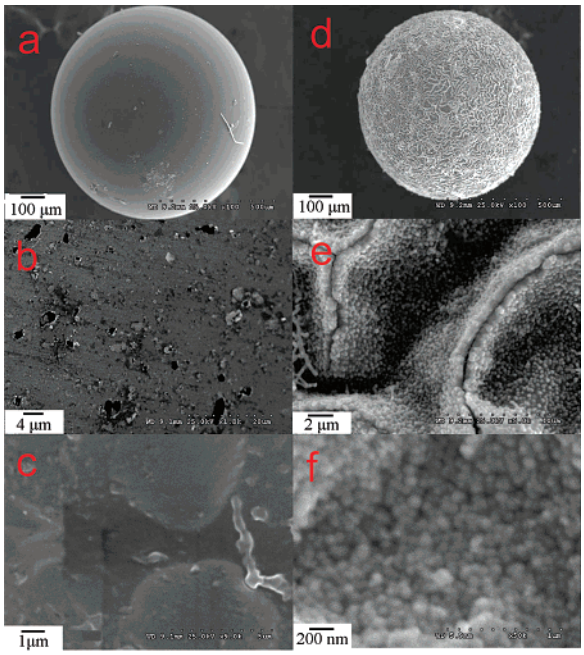

FIGURE 1. Scanning electron microscopy image of the exchanger resin (a−c) and the nanoscale ZVI particles immobilized on the resin (d−f).

An Agilent 6890N GC coupled with a Waters Micromass (Manchester, U.K.) AutoSpec Ultima mass spectrometer (HRGC/HRMS) was used to analyze four samples which had relatively high numbers of peaks. The GC had a 30 m × 0.1 μm film thickness DB-XLB column. The HRMS was operated at 35 eV ionization energy, and the resolution was 10 000.

Results and Discussion

Immobilization of n-ZVI on Resin. Figure 1 shows the scanning electron microscopy images of the ion-exchange resin particles. Before the immobilization of the n-ZVI, the surface of the resin was smooth (Figure 1a), except for some holes (Figure 1b) and unknown impurities (Figure 1c). Figure 1d−f shows the SEM images of the resin with n-ZVI particles immobilized on the resin surface. The ZVI particles formed from the reduction of Fe^{2+} were spherical, with majority being about 60 nm in diameter. These n-ZVI balls aggregated to form channels with a depth of about 3 μm and width of about 10 μm. It should be noted that these channels formed only with certain iron loadings. In our experiments, 0.01−0.07 g of iron/g of resin was found to be optimal. Below this range, the iron particles were scattered on the surface of the resin, and above the range, a smooth layer of iron formed. The formation of the channels is likely to increase the surface area of the material. In the experiments with BDE209, the resin with 0.056 g of iron/g of resin was used as stated above.

Kinetics. The results of this study clearly demonstrated that the debromination of BDE209 by nanoscale ZVI is rapid at ambient conditions and without the catalysis of noble metals. BDE209 disappeared after about 8 h (Figure 2). Regression of ln (C/C_0) versus time from 0 to 8 h is linear (R^2 = 0.93, p = 0.008, n = 5, Figure 3), resulting in a first-order rate constant of 0.28 ± 0.04 h^{-1} and a corresponding half-life of 2.5 h. The reactions are dramatically faster than the one observed by Keum and Li (*12*) using μ-ZVI powder (average diameter 15 μm, Aldrich), with which 92% of the BDE209 coated on the ZVI particles were removed after 40 days at room temperature. The enhanced reaction rate observed in this study with n-ZVI is most likely the result of the larger

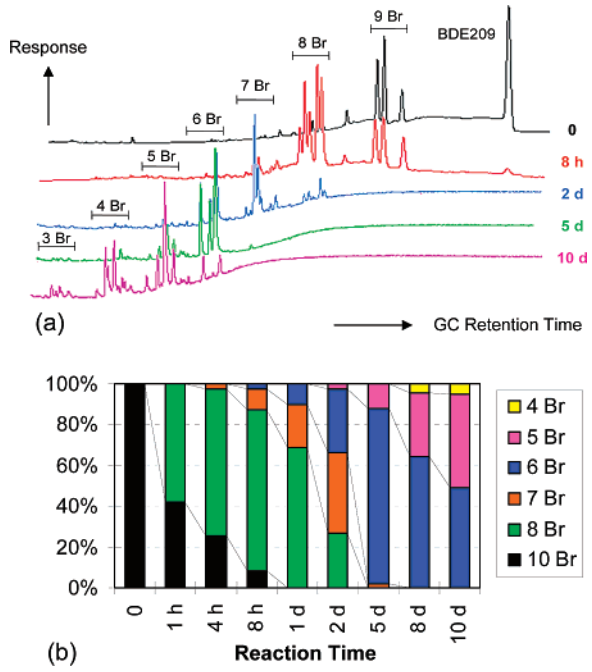

FIGURE 2. (a) GC-ECD chromatograms and (b) change in homolog distribution obtained at different reaction times. No debromination was observed in the control samples. In panel b, "8 Br" (green bars) is the sum of nonaBDEs and octaBDEs. The concentrations and molar fractions of nonaBDEs cannot be estimated because of the lack of chemical standards. The concentrations of some other congeners with no chemical standards were estimated assuming similar response factor with their isomers for which chemical standards were available. Average concentrations of replicates (n = 3) were calculated for each congener and then summed for each homolog. The average relative standard deviations (RSD) of the replicates were 29% (N = 148).

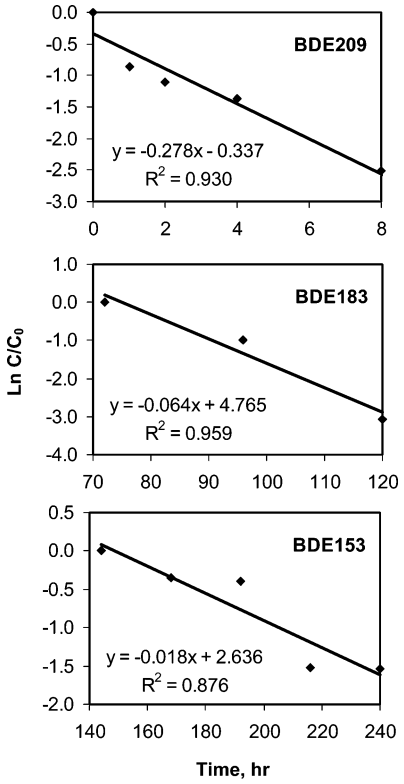

FIGURE 3. Pseudo-first-order kinetic plots for the disappearance of three PBDE congeners. For BDEs 183 and 153, the starting times are when the direct parent homologs could no longer be detected by GC-ECD.

surface areas of the particles. However, a quantitative comparison of reactivity between n-ZVI and μ-ZVI based on surface area-normalized reaction kinetics is not possible because the reactive surface area is difficult to estimate because of the attachment of the particles on resins. Other differences in experimental conditions and ZVI particle characteristics may also cause differences in reaction mechanisms or kinetics making a direct comparison between the two studies biased. In this work, the reaction took place in acetone/water mixtures; thus the observed rate could differ from those one can expect in pure water, natural waters, or wastewaters.

With the disappearance of BDE209, nona- through tri-BDEs formed in a sequential manner, as illustrated in Figure 2. No debromination of BDE209 was observed in control samples. Although chemical standards for nona-BDEs were not available, we are positive that the three peaks marked as "9-Br" are BDEs 208, 207, and 206 in the order of GC elution. They were detected in small amounts in the original technical product DE-83 as minor components, also in the control samples analyzed at all time intervals without noticeable increases relative to BDE209 with time. All three nona-BDEs appeared in significant amounts within 1 h, increased steadily for 8 h, and decreased to below detection in 24 h. There are 12 possible octa-BDEs, but only five major peaks were observed and confirmed by HRGC/HRMS. The sum of nona-BDEs and octa-BDEs was >50% of the total before approximately 12 h. The dominance shifted to hepta-BDEs after 2 days and, subsequently, to hexa-BDEs, which remained as the most abundant homolog group for days. After 10 days, penta-BDEs were present in significant amounts, and tetra-BDEs appeared. The recovery, as illustrated in Figure S3, tended to decrease over time, reflecting the difficulties in detecting and quantifying lower-brominated congeners with ECD. The possibility of forming non-BDE compounds cannot be ruled out. Overall, these results support the observation made by Keum and Li (*12*) that debromination of BDE209 is stepwise, with bromines being sequentially substituted by hydrogen.

The apparent overall reaction rate was continuously decreasing as the homolog distribution pattern shifted toward lower congeners. Because all congeners with 9 or fewer bromines may have acted as both daughter and mother at the same time, accurate determination of the congener specific rate constants from the results of this work is difficult. In Figure 3, kinetic plots were constructed for three congeners. Within the ranges of their respective time periods, the debromination of congeners appear to be kinetically first order, as shown by the linearity of the regressions. The pseudo-first-order rate constants, as indicated by the slopes, are obviously in the order of deca (BDE209) > hepta (BDE183) > hexa (BDE153).

As mentioned above, the dechlorination of PCB209 was much slower than that of BDE209. No dechlorination of PCB209 was noticeable when the experiment ended after 10 days using n-ZVI coated on resin. After 10 d of reaction with free n-ZVI particles suspended in solution, the added PCB209 decreased to approximately 21%. Meanwhile, the three nona-CBs increased from day 1 to 4, and then started to decrease. Five octa-CB peaks were observed, with their total concentration increasing throughout the 10 day experiments (Figure S2).

Identification of the Reaction Products. Identification of reaction products is critical in proposing the pathways and mechanisms. It is highly challenging, mainly because

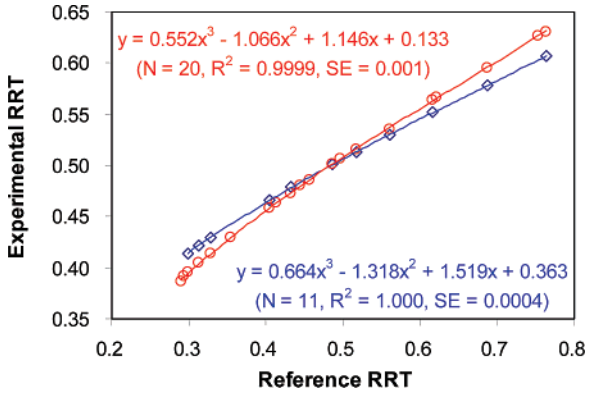

FIGURE 4. Regression of the experimental relative retention time (RRT) obtained in this work against the reference RRT reported in ref *17* for DB-5 column. Only tetra- through hepta-BDEs are included. RRT is defined as the retention time normalized by the sum of retention times of BDEs 47 and 183: red, PBDE standard EO5113 using 30 m DB-5 GC column and HRMS; blue, PBDE standard EO5103 using 60 m DB-5 GC column and ECD.

of the lack of PBDE standards at the time of the experiments. There were peaks with retention times that did not match any of the 43 chemical standards available in our laboratory. Third-order polynomial regression equations were obtained using the observed GC relative retention time (RRT) against an experimental reference RRT database for the DB-5 stationary phase (*23*). These equations (Figure 4) allowed us to increase the number of identifiable tetra- to hepta-congeners from 20 (in standard EO5113) to 84 (in the reference RRT database), although some congeners coelute. In addition, the HRMS was used to confirm the levels of bromination for the unknown peaks. Furthermore, quantitative structure retention relationships (QSRRs) previously developed from our work (*24*) and others (*25*) were also referred to in the identification of bromine-substitution patterns.

The three nona-BDEs were identified with confidence because their elution order is well established. Currently, individual standards are commercially available for only 7 out of 12 possible octa-BDEs. Two of the five observed octa-BDE peaks (Figure S1), the third and the fifth, were identified as BDEs 197 and 196, respectively, by matching retention times with chemical standards. BDE204, with a retention time slightly shorter than that of BDE197, was not found. The fourth peak matched the retention time of standard BDE203. BDE198 was reported to coelute on a 15 m column with BDE203 (*6*), and BDE199 has a predicted RRT that matches that of BDE198 (*25*); however, GC separation by the 30 m column did not produce additional peaks. The other two octa-BDE peaks could not be confidently determined because of the lack of chemical standards. Gerecke et al. (*6*) encountered the same problem and suggested that the first octa-BDE peak observed in their chromatogram was BDE202, which is believed to be the earliest eluting octa-BDE on commonly used nonpolar GC columns based on the lack of bromine at both para positions. Our observations do not contradict this possibility, and our QSRRs (*24*) also suggest that BDE202 elutes earlier than all other octa-BDEs. Although it is difficult to speculate the substitution pattern for the second octa-BDE peak, it is likely to be BDE201, which has only one para-bromine but all four ortho-bromines thus could elute earlier than BDE204, but less likely to be BDE200 which has a fully substituted ring (see below). None of the five observed octa-BDE peaks can represent BDE205, which elutes much later than BDE196 (*6*). It is noticed that the major peaks of octa-BDEs observed on GC chromatograms during degradation of BDE209 rarely exceeded five, as presented in several studies involving photochemical (*3*−*5*), biological (*26*), and microbial (*6*) debromination processes. The relative retention of the peaks suggests a possibility that a set of same octa-BDEs form when BDE209 naturally debrominates. In this work, we observed that the dechlorination of PCB209 by n-ZVI also generated five major octa-CB peaks, they were identified as PCBs 202, 204/200, 197, 201, and 196/203, by matching retention times with standards (Figure S2).

Three major and a few minor hepta-BDEs peaks were observed in this work. One major peak was confidently identified as BDE183, and another could be BDE181, although its retention time had shifted slightly (~0.04 min on 60 m column) when compared with standard. A major peak is suggested by the regression equations in Figure 4 to be BDE128, a hexa-BDE; however, this possibility is eliminated after confirmation by HRMS that the observed peak contains only hepta-BDEs. While the most closely matched hepta congener is BDE184, it may contain more than one congener which could not be separated even on the 60 m column and which is not in the RRT database (*23*). At least six major hexa-BDE congeners were formed, among them, BDEs 153 and 154 were identified. Another major peak eluted before and was only partially separated from BDE153 on the 60 m column was possibly congener 151 or 135 based on QSRR prediction (*24*). A broad peak between BDEs 154 and 153 may represent other but coeluting hexa-BDE congeners, which cannot be identified with confidence, although the closest match is BDE161 using the equations in Figure 4.

BDE99 is the only major penta-BDE congener that could be positively identified by matching retention times with standards. A major peak observed is believed to be BDE101 from application of the equations in Figure 4. There were four additional major penta-BDE peaks. One of them is suggested by the equation in Figure 4 to be BDE102, but the others cannot be identified. As the reaction proceeded, tetra- and tri-BDEs were produced with a number of congeners in each homolog. Although their accurate identifications became more difficult, BDE47, the most frequently detected in the environment, was confidently identified by matching retention time. Another major tetra-BDE peak had a retention time that matched BDE49, but complications arise because BDEs 49 and 68 share the same value of RRT (*23*).

Reaction Pathways. There is evidence that ortho chlorines are more resistant to elimination than meta and para chlorines in PCBs (*17*). In this work, we observed that, with the decrease of PCB209, the rate of formation was in the order CB208 > CB207 > CB206 (Figure S4b). Debromination of BDE209 resulted in the formation of all three nona-BDEs; however, their relative peak areas did not seem to differ much (Figure S4a). Keum and Li (*12*) used μ-ZVI with four PBDE congeners with 3−5 bromines and reported that the dominant degradation pathways were BDE28 (24−4) → BDE15 (4−4), BDE47 (24−24) → BDE28 (24−4), BDE66 (24−34) → BDE37 (34−4), and BDE100 (246−24) → BDE47 (24−24), where the numbers in parentheses refer to the bromine substitution positions on the two rings. The tenaciousness of para bromines is obvious. These observations are apparently in contrast to the positional preference observed for PCB, in which para chlorines are often the easiest to be removed, while ortho chlorines are more unyielding (*17*). In this work, confidently identified hepta- to penta-BDE products include 183, 153, 154, and 99; all retain both para bromines. However, the presence of unidentified peaks makes it difficult to conclusively confirm the positional preference or propose pathways.

The molar heat of formation H_f and the energy of the lowest-unoccupied molecular orbital (E_{LUMO}) have been found to correlate with the rate of dehalogenation of PCBs and PBDEs by ZVI (*12*, *17*). The general trends of increasing H_f and decreasing E_{LUMO} with increasing number of halogen

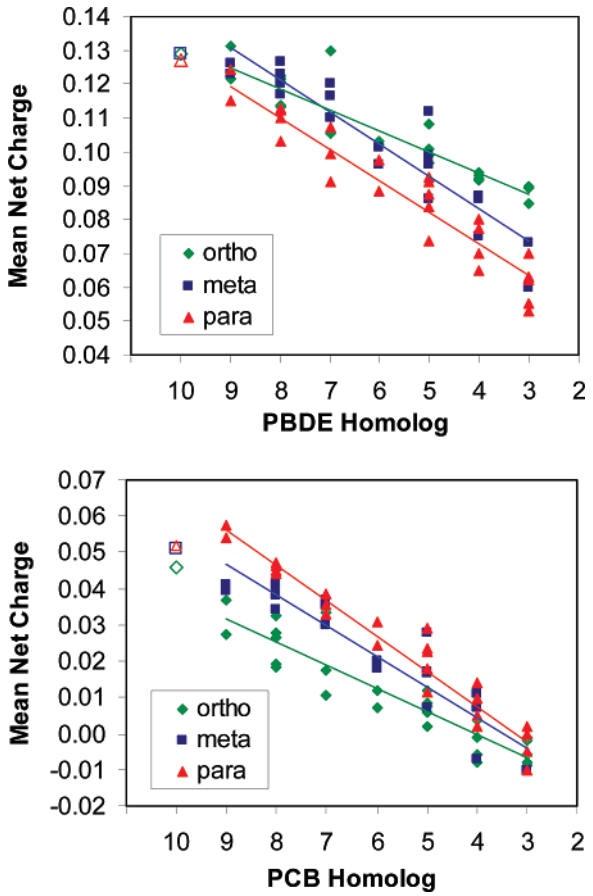

FIGURE 5. Mean net charges of individual halogen atoms in randomly selected (a) PBDE and (b) PCB molecules, calculated using the semiempirical AM1 method contained in the quantum chemical computation software HyperChem (release 7.0 for Windows). Those for deca congeners are drawn in empty symbols using the same color scheme for bromine-substitution positions and are not included in generating the regression lines.

atoms enable the establishment of correlations with the rate of dehalogenation among congeners in different homologs. However, the differences among isomers within a homolog may be more difficult to explain by such simple parameter correlations. Zeng et al. (*2*) found that PBDE congeners with one fully brominated phenyl ring are the least stable among isomers for penta, hexa, and hepta homologs. Indeed, all but one (BDE181, which is a minor hepta-BDE product) of the tetra- through hepta-BDE congeners identified in this work do not have fully substituted rings. The molecular energy levels of heavily brominated congeners may be more complex. In this work, among possible daughter congeners of BDE207 (23456-2346), BDEs 196 (2345−2346) and 197 (2346−2346) were found, while BDE204 (23456−246) was not. Although the presence of BDE203 (23456−245) is possible, it cannot be confirmed because of its known GC coelution with other congeners. If it is true for octa-BDEs that isomers with a fully brominated ring are less stable, we may speculate that the second octa-BDE peak in Figure S1 could be BDE201 (2346−2356) rather than BDE200 (23456−236).

Despite different stable conformations among congeners (*2*), the two rings in the PBDE molecules are roughly perpendicular to each other (*27*), making the molecules nonplanar and restricting the interactions between the two π-electron clouds. We therefore speculate that local structural or electronic descriptors, rather than molecular descriptors such as H_f, may better explain the positional preference of the debromination product formation. In this work, the net charges of individual atoms were calculated, using the semiempirical AM1 method contained in the quantum chemical computation software HyperChem (*28*), for the same sets of randomly selected congeners of PBDEs and PCBs. For PBDEs, the net charges are negative for all carbon atoms except the two connecting to the oxygen, while all bromines have positive charges. With few exceptions, para bromines have lower net charge than the meta and ortho bromines in the same ring (Figure 5a). In comparison, the net charges on chlorines in PCBs are lower (some are negative) than the corresponding bromines in PBDEs, and in contrast, para chlorines have higher net charge than ortho and meta chlorines in most cases (Figure 5b). For fully substituted congeners, the average net charges of para, meta, and ortho halogens are close, and the ranks are ortho > meta > para in BDE209 and para ≈ meta > ortho in PCB209. As we observed in this work (Figure S4b), PCB208 had the highest rate of formation through dropping a para chlorine from PCB209, while PCB206, which forms when an ortho chlorine drops, had the lowest rate.

In addition, the modeling results in Figure 5 seem to suggest that the differences in net charges among halogen atoms at different positions tend to increase as the degree of chlorination increases from 3 to 9 for PCBs, but such a trend is not obvious and could be opposite for PBDEs. These results are not different if the two rings are separately plotted and individual values are used rather than the averages (Figure S5). However, experimental observations of this and other studies are not sufficient to confirm these trends.

Although other factors such as steric effect may also play a role, the net charge may be a useful descriptor in the investigation of the relative reactivity among isomers and in conceptualization and comparison of the mechanisms of the dehalogenation processes for PCBs and PBDEs, as well as other halogenated organic chemical groups. Because the number and positions of halogen atoms in PCBs and PBDEs largely decide their toxicity, knowledge on dehalogenation pathways is important to the assessment of ecotoxicity and human health effect. As such, further investigation is warranted.

Acknowledgments

This work was jointly supported by the National Basic Research Program of China (2003CB415001) and the National Natural Science Foundation of China (20621703).

Supporting Information Available

Additional tables and figures. This material is available free of charge via the Internet at http://pubs.acs.org.

Literature Cited

(1) Laguardia, M. J.; Hale, R. C.; Harvey, E. Detailed polybrominated diphenyl ether (PBDE) congener composition of the widely used penta-, octa-, and deca-PBDE technical flame-retardant mixtures. *Environ. Sci. Technol.* **2006**, *40*, 6247−6254.

(2) Zeng, X.; Freeman, P. K.; Vasil'ev, Y. V.; Voinov, V. G.; Simonich, S. L.; Barofsky, D. F. Theoretical calculation of thermodynamic properties of polybrominated diphenyl ethers. *J. Chem. Eng. Data* **2005**, *50*, 1548−1556.

(3) Eriksson, J.; Green, N.; Marsh, G. Photochemical decomposition of 15 polybrominated diphenyl ether congeners in methanol/water. *Environ. Sci. Technol.* **2004**, *38* (11), 3119−3125.

(4) Bezares-Cruz, J.; Jafvert, C. T.; Hua I. Solar photodecomposition of decabromodiphenyl ether: products and quantum yield. *Environ. Sci. Technol.* **2004**, *38* (15), 4149−4156.

(5) Söderström, G.; Sellström, U.; de Wit, C. A.; Tysklind, M. Photolytic debromination of decabromodiphenyl ether (BDE 209). *Environ. Sci. Technol.* **2004**, *38*, 127−132.

(6) Gerecke, A. C.; Hartmann, P. C.; Heeb, V.; Kohler, H-P. E.; Giger, W.; Schmid, H.; Zennegg, M.; Kohler, M. Anaerobic degradation of decabromodiphenyl ether. *Environ. Sci. Technol.* **2005**, *39*, 1078−1083.

(7) He, J-Z.; Robrock, K.; Alvarez-Cohen, L. Microbial reductive debromination of polybrominated diphenyl ethers (PBDEs). *Environ. Sci. Technol.* **2006**, *40*, 4429−4434.
(8) ATSDR. *Toxicological Profile for Polybrominated Biphenyls and Polybrominated Diphenyl Ethers (PBBs and PBDEs)*; U.S. Department Of Health and Human Services, The Agency for Toxic Substances and Disease Registry (ATSDR): Washington, DC, 2004; http://www.atsdr.cdc.gov/toxprofiles/tp68.html (accessed in December, 2006).
(9) Pakdeesusuk, U.; Jones, W. J.; Lee, C. M.; Garrison, A. W.; O'Niell, W. L.; Freedman, D. L.; Coates, J. T.; Wong, C. S. Changes in enantiomeric fractions during microbial reductive dechlorination of PCB132, PCB149, and Aroclor 1254 in Lake Hartwell sediment microcosms. *Environ. Sci. Technol.* **2003**, *37*, 1100−1107.
(10) Bedard, D. L.; May, R. J. Characterization of the polychlorinated biphenyls in the sediments of woods pond: Evidence for microbial dechlorination of Aroclor 1260 in situ. *Environ. Sci. Technol.* **1996**, *30*, 237−245.
(11) Quensen, J. F.; Tiedje, J. M.; Boyd, S. A. Reductive dechlorination of polychlorinated biphenyls by anaerobic microorganisms from sediments. *Science* **1988**, *242*, 752−754.
(12) Keum, Y-S.; Li, Q. X. Reductive debromination of polybrominated diphenyl ethers by zerovalent iron. *Environ. Sci. Technol.* **2005**, *39* (7), 2280−2286.
(13) Gardner, K. *In-Situ Treatment of PCBs in Marine and Freshwater Sediments Using Colloidal Zero-Valent Iron*; Final Report to the Cooperative Institute for Coastal and Estuarine Environmental Technology (CICEET); Cooperative Institute for Coastal and Estuarine Environmental Technology: Durham, NH, 2004; http://rfp.ciceet.unh.edu/display/report.php?chosen=51 (accessed on May 20, 2007).
(14) Varanasi, P.; Fullana, A.; Sidhu, S. Remediation of PCB contaminated soils using iron nano-particles. *Chemosphere* **2007**, *66*, 1031−1038.
(15) Wang, C. B.; Zhang, W. X. Synthesizing nanoscale iron particles for rapid and complete dechlorination of TCE and PCBs. *Environ. Sci. Technol.* **1997**, *31*, 2154−2156.
(16) Chuang, F. W.; Larson, R. A.; Wessman, M. S. Zero-valent iron-promoted dechlorination of polychlorinated biphenyls. *Environ. Sci. Technol.* **1995**, *29*, 2460−2463.
(17) Yak, H. K.; Lang, Q. Y.; Wai, C. M. Relative resistance of positional isomers of polychlorinated biphenyls toward reductive dechlorination by zerovalent iron in subcritical water. *Environ. Sci. Technol.* **2000**, *34*, 2792−2798.
(18) Yak, H. K.; Wenclawiak, B. W.; Cheng, I. F.; Doyle, J. G.; Wai, C. M. Reductive dechlorination of polychlorinated biphenyls by zerovalent iron in subcritical water. *Environ. Sci. Technol.* **1999**, *33*, 1307.
(19) Kim, Y. H.; Shin, W. S.; Ko, S. H. Reductive dechlorination of chlorinated biphenyls by palladized zero-valent metals. *J. Environ. Sci. Health* **2004**, *A39* (5), 1177−1188.
(20) Lowry, G. V.; Johnson, K. M. Congener-specific dechlorination of dissolved PCBs by microscale and nanoscale zerovalent iron in a water/methanol solution. *Environ. Sci. Technol.* **2004**, *38* (19), 5208−5216.
(21) Oberdörster, G.; Oberdörster, E.; Oberdörster, J. Nanotoxicology: An emerging discipline evolving from studies of ultrafine particles. *Environ. Health Perspect.* **2005**, *113*, 823−839.
(22) The Royal Society. Nanoscience and nanotechnologies: Opportunities and uncertainties. http://www.nanotec.org.uk/finalReport.htm (accessed July 9, 2006).
(23) Korytár, P.; Covaci, A.; de Boer, J.; Gelbin, A.; Brinkman, U. A. Th. Retention-time database of 126 polybrominated diphenyl ether congeners and two Bromkal technical mixtures on seven capillary gas chromatographic columns. *J. Chromatogr. A* **2005**, *1065*, 239−249.
(24) Wang, Y. W.; Li, A.; Liu, H. X.; Zhang, Q. H.; Ma, W. P.; Song, W. L.; Jiang, G. B. Development of quantitative structure gas chromatographic relative retention times models on different stationary phases for 209 polybrominated diphenyl ether congeners. *J. Chromatogr. A.* **2006**, *1103*, 324−328.
(25) Rayne, S.; Ikonomou, M. G. Predicting gas chromatographic retention times for the 209 polybrominated diphenyl ether congeners. *J. Chromatogr. A* **2003**, *1016*, 235−248.
(26) Stapleton, H. M.; Brazil, B.; Holbrook, R. D.; Mitchelmore, C. L.; Benedict, R.; Konstantinov, A.; Potter, D. In vivo and in vitro debromination of decabromodiphenyl ether (BDE209) by juvenile rainbow trout and common Carp. *Environ. Sci. Technol.* **2006**, *40*, 4653−4658.
(27) Wang, Y. W.; Liu, H. X.; Zhao, C. Y.; Liu, H. X.; Cai, Z. W.; Jiang, G. B. Quantitative structure−activity relationship models for prediction of the toxicity of polybrominated diphenyl ether congeners. *Environ. Sci. Technol.* **2005**, *39*, 4961−4966.
(28) *HyperChem*, release 7.0 for Windows; Hypercube, Inc.: Gainesville, Fl, 2002.
(29) Mullin, M. D.; Pochini, C. M.; McCrindle, S.; Romkes, M.; Safe, S. H.; Safe, L. M. High resolution PCB analysis: synthesis and chromatographic properties of all 209 PCB congeners. *Environ. Sci. Technol.* **1984**, *18*, 468−476.

Received for review April 1, 2007. Revised manuscript received July 18, 2007. Accepted July 19, 2007.

ES070769C